A Dual Planar Reflectarray With Synthesized Phase and Amplitude Distribution

Ralf Leberer and Wolfgang Menzel, *Fellow, IEEE*

***Abstract*—A quasi-planar reflector arrangement for generating an arbitrary phase and amplitude distribution in the antenna aperture and thus a wide range of far field patterns is presented. A parallel pair of reflectarrays is used. One is implemented as a standard reflectarray using rectangular patches on a microwave substrate with metallized backside. The other reflectarray is provided with a polarizing grid, which acts as a ground plane for one polarization and is transparent for the orthogonal polarization. An offset rectangular feed horn is embedded in the lower reflectarray to illuminate the upper reflector. A design procedure for a linear polarized antenna with a sector beam in the azimuth and a narrow beam width in the elevation is presented and is verified with measurement results.**

***Index Terms*—Array signal processing, millimeter wave antenna arrays, multireflector antennas, planar arrays, shaped beam antennas.**

I. Introduction

In the last decade the interest in reflectarrays has increased significantly. Standard technologies are used to produce low-cost planar reflectors with good reproducibility. Low weight, easy mounting, and small reflector thickness make them attractive for a wide range of applications. In [1]–[3], shaped-beam planar reflector antennas have been presented for coverage of the European, South American, or Australian continent, respectively. Various planar reflectors with frequency-selective surfaces have been used in [4] to modify the polarization and beam shape of sector and omnidirectional antennas in the 60 GHz band. A local multipoint distribution service base-station antenna with sectorial cosecant squared beam has been presented in [5] using a multilayer folded reflectarray.

All these shaped-beam antennas use phase-only control to generate a desired pattern in the far field of a planar reflectarray, while the amplitude distribution along the array is prefixed by the feeding element. Since commonly waveguide horns are used to illuminate the reflectarray, the variation of the array amplitude distribution is very limited and has to be accepted to be inflexible. The use of an additional subreflector does not improve the flexibility significantly, as subreflectors are usually electrically small and the radii of curvature limited. Moreover, the side lobes and gain are affected by subreflector blocking.

In this paper, a dual planar reflector combination is used to control, in addition to the phase, the amplitude distribution in the aperture of a two-dimensional reflectarray. With this additional degree of freedom, the complex amplitude distribution in the reflector aperture can be optimized for the shape of even more complex radiation patterns, low side lobes, and high antenna gain, and the influence of fabrication tolerances can be reduced.

Manuscript received February 24, 2005; June 18, 2005.

R. Leberer is with the European Aeronautic Defence and Space (EADS) Company Deutschland GmbH, 89077 Ulm, Germany (e-mail: ralf.leberer@eads.com).

W. Menzel is with the Microwave Techniques Department, University of Ulm, Ulm 89081, Germany.

Digital Object Identifier 10.1109/TAP.2005.858813

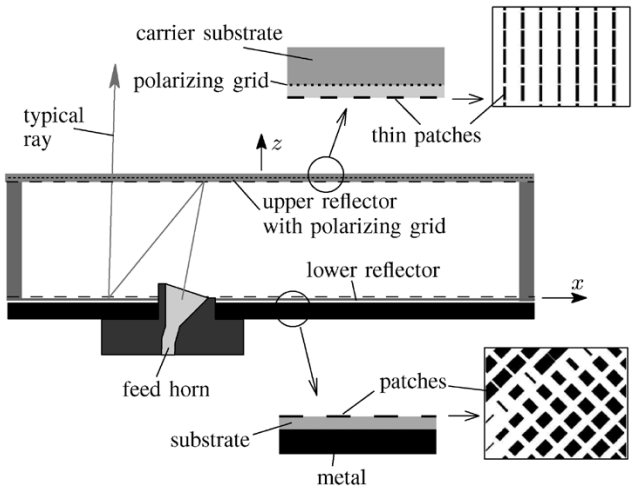

Fig. 1. Cross-section of a dual-reflectarray setup.

The combination of the feed and the upper reflector forms a reflectarray with fixed amplitude distribution, as known from conventional reflectarrays. Using instead a semitransparent reflectarray and combining it with a second reflectarray, new possibilities for beam forming with arbitrary phase and amplitude distribution arise.

II. Basic Principle of the Dual Reflector Combination

The basic cross-section of a dual-reflectarray antenna is sketched in Fig. 1 The setup is in principle similar to a folded reflector antenna [6]–[8] and differs only in the polarizing grid or the upper reflector, respectively. It consists of a waveguide horn, the upper reflector with polarizing grid, and the lower reflector. The radiation from the feed is polarized in such a way that it is reflected by the upper dual-layer reflector. There is a printed grid between the two layers and thin patches/dipoles on the lower side of the upper reflector, which are oriented in the direction of the grid (Figs. 1 and 2). The overall thickness of the two substrates is about half a wavelength, so the structure is (almost) transparent for the orthogonal polarization, which is hardly affected by the dipoles and the grid. As demonstrated in [9], the printed grid can be used as a ground plane of the reflectarray for the parallel polarization, and the wave is reflected with a phase that depends on the specific dipole lengths. As the grid dimensions are capillary compared to the wave length

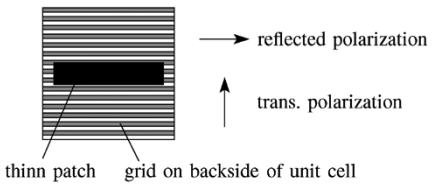

Fig. 2. Cell of the upper reflector with a thin dipole and a grid on the substrate backside, which acts as a ground plane for horizontal polarization and is transparent for orthogonal polarization.

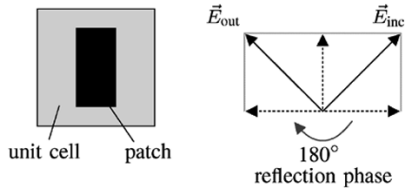

Fig. 3. Ninety degree twist of polarization using cells with 180° difference in reflection phases of orthogonal field components.

and to the patch dimensions, the reflection phase of the unit cell is the same for a ground plane and an appropriate grid. In this paper, the upper reflectarray is used to modify the direction of the reflected rays in such a way that the desired amplitude distribution on the lower reflector is generated.

The lower reflector is made up of a substrate with a ground plane on the backside and printed rectangular patches on the upper side. The patch axes of this array are tilted by 45° with respect to the incident electric field. The electric field vector can be decomposed into the two components parallel to the patch axes, and the reflection properties can be determined separately. The dimensions of the patches are selected in such a way that a phase difference of 180° occurs between the reflection phase of these two components. Superposition of the reflected field components then leads to a twisting of the polarization by 90° (Fig. 3). The necessary 180° reflection phase difference between the two field components of the reflected wave can be achieved for a large number of combinations of length and width of the patches differing by their absolute reflection phase. This degree of freedom now is used to adjust the required reflection phase and synthesize the desired phase distribution of the reflected wave. The reflected wave adjusted in amplitude and phase distribution passes the upper reflector undisturbed, as the grid is transparent for this polarization as has been discussed above.

As has been shown in [6]–[8], the polarization twisting with additional phase adjust can be performed over a wide bandwidth (several gigahertz bandwidth at 60 GHz). Compared to a nontwisting reflectarray with linear polarization, the reflection phase of a unit cell is theoretically more sensitive to deviations of the patch geometry or to frequency shifts. Phase errors not only cause deformations of the phase front but also generate unwanted polarization proportions, which could cause undefined side lobes. Reflection phase errors of the x and y components contribute to the overall deviation. These deviations are typically caused by fabrication tolerances or frequency offsets from the design frequency. As the errors of both components are usually about the same size or at least have the same sign, experimental results have shown that the overall error is marginally higher than with nonfolded reflectarrays.

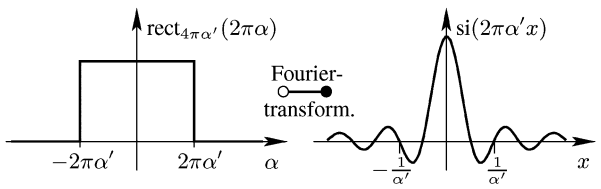

Fig. 4. Idealized sector characteristic with sector angle $\Delta\theta(\alpha' = \sin(\Delta\theta/2)/\lambda, \alpha = \sin\theta/\lambda)$ and si-shaped amplitude distribution, which is its Fourier transform.

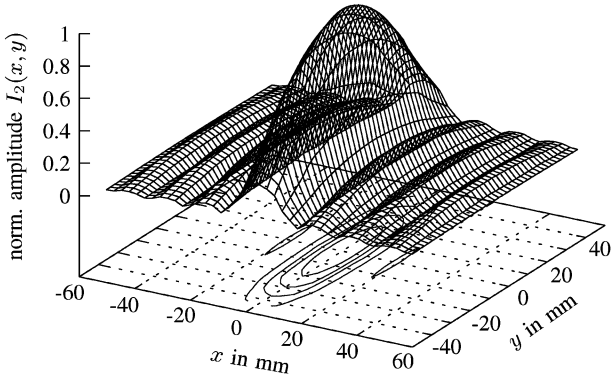

Fig. 5. Normalized amplitude distribution I_2 on the lower reflector with |si|-distribution along the x axis and cosine taper along the y axis.

III. Design of a Sector-Beam Antenna

A. Complex Amplitude Distribution

The complex amplitude in the antenna aperture can be obtained from the inverse Fourier transform of the far field pattern. Numerous techniques have been presented to optimize this complex amplitude distribution with respect to tolerances, malfunction of single elements, the desired far field pattern, and requirements of specifications [10]–[16].

In this paper, a sector-beam antenna with narrow beamwidth in the elevation is designed. A sector-beam can be described with a rect-function as shown in Fig. 4 The Fourier transformation of this distribution is a si-function ($\text{si}(x) = \sin x/x$). For the designed antenna, a rectangular aperture with a si-shaped amplitude distribution along the x-axis and a cosine-shaped distribution along the y axis is chosen as shown in Fig. 5

$$I_2(x,y) = |\text{si}(ax)|\cos(\text{by}) \tag{1}$$

with the constants a, b and the coordinates on the lower reflector x, y (index 1 is used for the upper reflector; index 2 for the lower reflector). The negative amplitude values are replaced by absolute values but with a phase shift of 180°, which is included in the phase adjustment of the lower reflector. Thus for the si-distribution, only the two absolute phase values 0° and 180° have to be included in the phase adjustment, alternating along the x axis at each zero of the si-function. In case of any other complex amplitude distribution, these values can be synthesized in the same way. As the dimensions of the reflector are restricted, in this paper the si-distribution is cut after the fourth zero in positive and negative direction of the function (Fig. 5).

To minimize the aperture blocking, the feed is placed in a region in the lower reflector plane with low power density. A suitable position is the first zero of the si-distribution along the

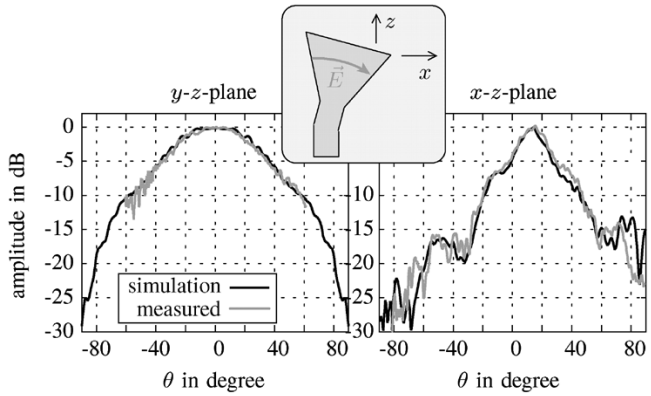

Fig. 6. Far field characteristic of the rectangular feed horn in the H- and E-plane at 58 GHz.

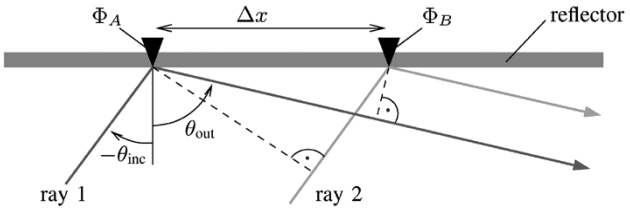

Fig. 7. Reflection of rays at a one-dimensional reflector with frequency-selective surfaces.

x axis. As the desired amplitude distribution I_2 is more concentrated to the center along the x axis than along the y axis, a rectangular feed with smaller beam width in the x-z plane than in the y-z plane is chosen (Fig. 6). Thus the maximum slope of the reflection phase on the upper reflector is reduced.

B. Law of Reflection for Frequency-Selective Surfaces

Choosing the appropriate reflection phase distribution $\Phi_1(x,y)$ of the upper reflectarray, the rays are reflected in such a way that the amplitude distribution $|I_1(x,y)|$ on the upper reflector, which is originated by the feed illumination, is mapped to the distribution $|I_2(x,y)|$ on the lower reflector (Fig. 5). The reflection phase $\Phi_1(x,y)$ for the desired mapping $I_1 \rightarrow I_2$ can be calculated introducing the law of reflection for frequency selective surfaces.

For a one-dimensional or rotation-symmetrical reflector, the law of reflection can be derived regarding two rays, which are reflected on a frequency-selective surface with reflection phases Φ_A and Φ_B, as shown in Fig. 7. For the case $\Phi_A \neq \Phi_B$, the incident angle $-\theta_{\rm inc}$ of the rays is not equal to the angle of the reflected rays $\theta_{\rm out}$. The phases and angles have to fulfill the condition

$$-\Delta x \cdot \sin\theta_{\rm out} + \frac{1}{k}\Phi_A = \Delta x \cdot \sin\theta_{\rm inc} + \frac{1}{k}\Phi_B \qquad (2)$$

to get constructive superposition of the reflected rays. Assuming a continuous differentiable reflection phase $\Phi(x)$ and $\Delta x \rightarrow 0$, (2) can be written as

$$\sin\theta_{\rm out} + \sin\theta_{\rm inc} = -\frac{1}{k}\frac{\partial\Phi(x)}{\partial x}. \qquad (3)$$

For a two-dimensional reflector, the y dimension has to be considered in the same way, and the two equations

$$\sin\theta_{\rm out}\cos\phi_{\rm out} + \sin\theta_{\rm inc}\cos\phi_{\rm inc} = -\frac{1}{k}\frac{\partial\Phi(x,y)}{\partial x} \qquad (4)$$

$$\sin\theta_{\rm out}\sin\phi_{\rm out} + \sin\theta_{\rm inc}\sin\phi_{\rm inc} = -\frac{1}{k}\frac{\partial\Phi(x,y)}{\partial y} \qquad (5)$$

describe the interrelationship between the incident angles $\theta_{\rm inc}, \phi_{\rm inc}$, the reflection phase $\Phi(x,y)$, and the direction of the rays after the reflection $\theta_{\rm out}, \phi_{\rm out}$, respectively.

C. The Law of Energy Conservation

With (4) and (5), the path of rays can be calculated for a given reflection phase $\Phi_1(x,y)$ but no information about the power density along the rays is given. With the law of energy conservation, an interrelationship between the amplitude distributions I_1 and I_2 on the upper and lower reflector is given. This can be written in differential form as

$$\frac{{\rm d}x_2{\rm d}y_2}{{\rm d}x_1{\rm d}y_1} = \frac{I_1^2(x_1,y_1)}{C^2 I_2^2(x_2,y_2)} \qquad (6)$$

with points (x_1,y_1) and (x_2,y_2) on the upper and lower reflector, respectively. C is a normalization factor that can be calculated from

$$C^2 = \frac{\int_{x_{1,\min}}^{x_{1,\max}}\int_{y_{1,\min}}^{y_{1,\max}} I_1^2(x_1,y_1){\rm d}y_1{\rm d}x_1}{\int_{x_{2,\min}}^{x_{2,\max}}\int_{y_{2,\min}}^{y_{2,\max}} I_2^2(x_2,y_2){\rm d}y_2{\rm d}x_2} \qquad (7)$$

with the minimum and maximum reflector extents $x_{1,\min/\max}, y_{1,\min/\max}$ and $x_{2,\min/\max}, y_{2,\min/\max}$. The power reflected from a small rectangle ${\rm d}y_1{\rm d}x_1$ on the upper reflector is mapped to a rectangle ${\rm d}y_2{\rm d}x_2$ on the lower reflector. The relation of the power densities I_1^2/I_2^2 on the corresponding positions on the reflectors is equivalent to the inverse relation of the rectangle sizes ${\rm d}y_2{\rm d}x_2/{\rm d}y_1{\rm d}x_1$.

D. Calculation of Reflection Phases $\Phi_1(X,Y)$ and $\Phi_2(X,Y)$ on the Upper and Lower Reflector

With the law of reflection [(4) and (5)] and the law of energy conservation [(6)], a set of differential equations is given. Substituting the angles $\theta_{\rm inc}, \phi_{\rm inc}, \theta_{\rm out}$, and $\phi_{\rm out}$ in (4) and (5), the course of the rays $x_2(x_1,y_1), y_2(x_1,y_1)$ and the reflection phase $\Phi_1(x_1,y_1)$ on the upper reflector is obtained. These angles can be described in terms of geometrical dimensions

$$\tan\theta_{\rm inc} = \frac{\sqrt{(x_1 - x_{\rm feed})^2 + y_1^2}}{h} \qquad (8)$$

$$\tan\phi_{\rm inc} = \frac{y_1}{x_1 - x_{\rm feed}} \qquad (9)$$

$$\tan\theta_{\rm out} = \frac{\sqrt{(x_2 - x_1)^2 + (y_2 - y_1)^2}}{h} \qquad (10)$$

$$\tan\phi_{\rm out} = \frac{(y_2 - y_1)}{(x_2 - x_1)} \qquad (11)$$

with the offset feed position $(x_{\rm feed}, 0)$ and the distance h between the two parallel reflectors.

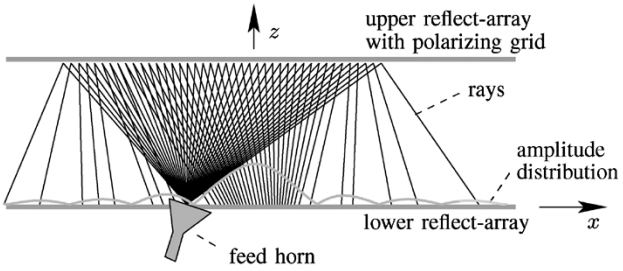

Fig. 8. Rays in the x-z plane.

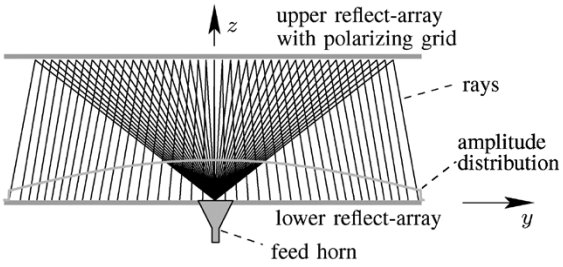

Fig. 9. (Projected) rays in the y-z plane.

For an axially symmetric setup and field configuration, the three unknowns can be extracted directly from the three differential equations. In case of an arbitrary two-dimensional phase distributions Φ_1 and Φ_2, only an approximate solution is found, comparable to dual optical reflector configurations [17].

For amplitude distributions I_1 and I_2 which can be described by separable functions in x and y, such as I_2 and (approximately) I_1 in this example, the equations can be easily solved applying an additional mapping restriction. This restriction can be substituted in the integral form of (6), e.g.,

$$C^2 \int_{x_{2,\min}}^{x_2} \int_{y_{2,\min}}^{y_{2,\max}} I_2^2(x_2, y_2) \mathrm{d}y_2 \mathrm{d}x_2 = \int_{x_{1,\min}}^{x_1} \int_{y_{1,\min}}^{y_{1,\max}} I_1^2(x_1, y_1) \mathrm{d}y_1 \mathrm{d}x_1. \quad (12)$$

All rays being reflected at the upper reflector at the x position x_1 are reflected on the lower reflector at the x position x_2, independent from the y position. Thus from (12), a mapping function $x_2(x_1)$ is obtained. With this function and (6), a function $y_2(x_1, y_1)$ can be derived. The rays of the sector beam antenna in the x-z and y-z plane are shown in Figs. 8 and 9, respectively. Along the $x$axis, the rays are concentrated in the center of the lower reflector to generate a si-shaped power distribution.

Now knowing the course of the rays, the required reflection phase $\Phi_1(x_1, y_1)$ is determined integrating (4) and (5). Choosing appropriate integration constants, the reflection phase $\Phi_1(x_1, y_1)$ may be calculated as shown in Fig. 10.

The reflection phase on the lower reflector is chosen to compensate the (electrical) length of the rays from the phase center of the feed to the lower reflector and to adjust the appropriate phase value of 0° or 180° for positive or negative values of the si-function. Additionally, the polarization twist is performed choosing patches with 180° reflection phase difference between the orthogonal polarizations.

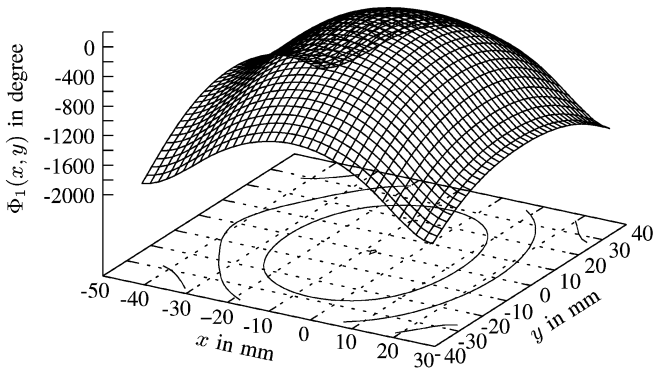

Fig. 10. Calculated reflection phase $\Phi_1(x_1, y_1)$ on the upper reflector.

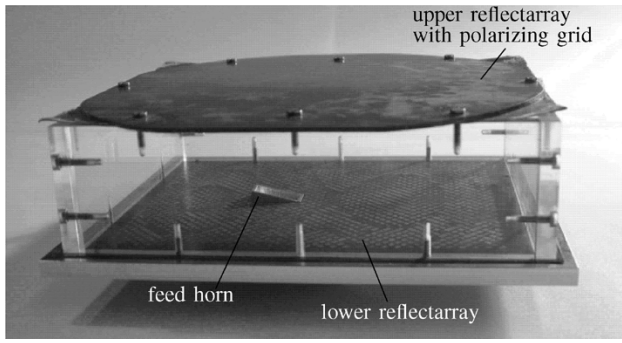

Fig. 11. Photograph of the fabricated double-reflectarray.

IV. Realization of the Antenna

A 24° sector beam antenna with small beam width in the elevation has been realized at 58 GHz. A photograph of the fabricated double-reflectarray is shown in Fig. 11. The two reflectors are fixed at a distance of 25 mm on a rectangular acryl-frame.

The rectangular feed horn is fixed on a rectangular aluminum plate. The horn has an aperture of 14 mm × 6 mm and is inclined by 13° to the z axis in the $x-z$ plane, as has been described in Section III-A. Degradation of the far field characteristic could generally be caused by cross-polarized portions of the feed radiation, leaking directly through the polarizing grid. This can, however, be neglected due to the fact that a feed horn with low cross-polarization (<-23 dB) has been chosen for the present design.

For the lower reflector, a 130 mm × 95 mm × 0.254 mm RT/duroid 5880 substrate with $\epsilon_r = 2.2$ is used. There are about 1660 rectangular patches with 2.2 mm × 2.2 mm cell size on it. The upper reflector consists of two 0.254- and 1.41-mm-thick substrates, both with permittivity $\epsilon_r = 2.2$ and with a polarizing grid (0.1 mm strip width, 0.25 mm lattice constant) in between. Fig. 2 shows that 1440 thin patches are placed on the thinner layer in the direction of the grid stripes.

The cells on the upper and lower reflector do not cover the full 360° reflection phase range. Only about 89% and 79% of the reflection phase values on the upper and lower reflector, respectively, can be generated with the single layer structure. Unrealizable phase values have been approached with the closest available value, causing local discrepancies from the desired course of the rays. Choosing an appropriate phase offset for all cells, the overall deviations can be minimized.

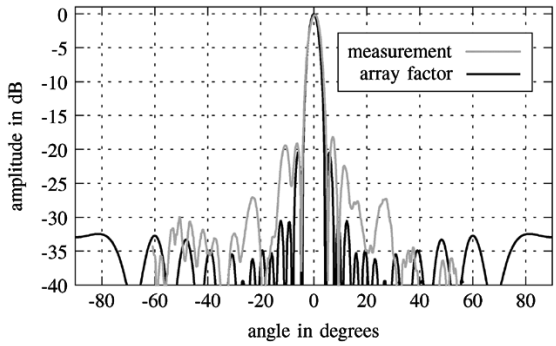

Fig. 12. Normalized measured and simulated far field characteristic in the E-plane (pencil beam) at 57.6 GHz.

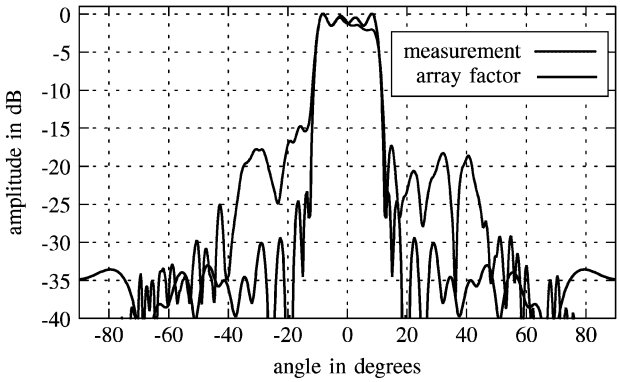

Fig. 13. Normalized measured and simulated far field characteristic in the H-plane (sector beam) at 57.6 GHz.

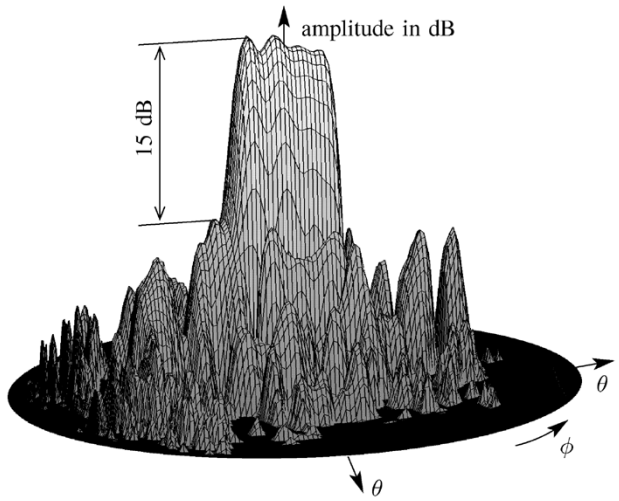

Fig. 14. Measured normalized far field characteristic at 57.6 GHz from −35 to 0 dB.

V. Measurement Results

The measurement results show good agreement with the simulated array factor in the E- and H-plane (Figs. 12 and 13). Only in the sector-plane, side lobes arise up to −15 dB, mainly due to amplitude and phase deviations of single cells from the nominal value, effectuated by fabrication tolerances or rounded reflection phase values, as explained in Section IV. Outside of this main plane, the side lobes are much lower (Fig. 14).

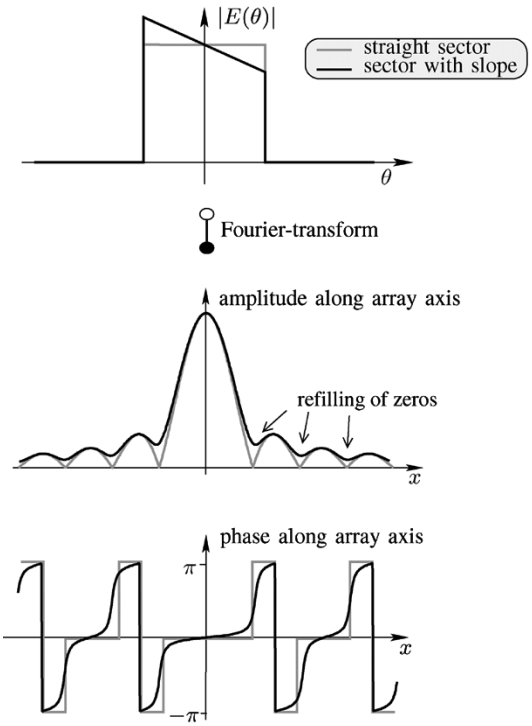

Fig. 15. Sector slope caused by inaccurate phase and amplitude reproduction.

The inclination of the sector characteristic between ±12° is caused by a unwanted curvature of the upper reflector in the experimental setup and "refilling" of the si-function zeros due to suboptimal realization of the desired amplitude and phase distribution as demonstrated in Fig. 15. The distributions have to fulfill the Nyquist condition as they are represented by a discrete array. Thus the distributions chosen for this example can only be synthesized approximated as the array constant does not fulfill the nyquist condition completely. Other distributions, unlike the rectangular phase distribution and the undifferentiable amplitude distribution ($|\mathrm{si}|$), can be synthesized much more precisely, and even better results are expected.

The antenna bandwidth is limited by the narrow-band behavior of the two reflectarrays. Within a bandwidth of more than 1 GHz, which is sufficient for many applications, the inclination of the sector and the side lobes are small. The pencil characteristic changes only marginally over the frequency. In the sector plane, the sector slope increases at higher frequencies and decreases at lower frequencies. The side lobes arise at lower frequencies and decrease at higher frequencies in a ±1 GHz frequency range.

Due to tolerances in the etching process of the substrates, the patch dimensions of the realized reflectors are on average about 25 μm larger than the nominal value. This results in a 0.4 GHz shift to lower frequencies and to deviations from the simulated far field pattern.

VI. Conclusion

A new double-reflector arrangement for synthesizing phase and amplitude distribution along a planar reflectarray has been presented. A combination of a reflectarray and a polarizing grid has been used to generate the desired amplitude distribution on

the lower reflectarray, which is used to twist the polarization and to adjust the phase. As the upper reflector has about the same size as the lower reflector, the desired amplitude distribution can be synthesized in much more detail than with an electrically small subreflector, which is usually used in optical reflector setups. The law of reflection for frequency-selective surfaces is introduced, and a design procedure for reflection phases of the two reflectors using the law of energy conservation is presented. A sector-beam antenna is designed and results are verified by measurements.

REFERENCES

[1] D. M. Pozar, S. D. Targonski, and R. Pokuls, "A shaped-beam microstrip patch reflectarray," *IEEE Trans. Antennas Propag.*, vol. 47, pp. 1167–1173, Jul. 1999.

[2] J. A. Encinar and J. A. Zornoza, "Three-layer printed reflectarrays for contoured beam space applications," *IEEE Trans. Antennas Propag.*, vol. 52, pp. 1138–1148, May 2004.

[3] J. A. Zornoza, J. A. Encinar, and M. E. Bialkowski, "A double-layer microstrip reflectarray design to obtain Australia and New Zealand footprint," in *Proc. IEEE Antennas Propagation Soc. Int. Symp.*, vol. 3, Jun. 22–27, 2003, pp. 310–313.

[4] R. Leberer and W. Menzel, "Folded millimeter-wave shaped-beam reflectarrays," in *Proc. Topical Symp. Millimeter Waves (TSMMW)*, Yokusuka, Japan, Mar. 26–27, 2004, pp. 93–97.

[5] J. A. Zornoza, R. Leberer, M. Moraga, J. A. Encinar, and W. Menzel, "A folded 3-layer printed reflectarray with shaped pattern for LMD's central station sectored antenna," in *Proc. IEEE Int. Symp. Antennas Propagation*, vol. 1, Monterey, CA, Jul. 2004, pp. 5–8.

[6] W. Menzel, D. Pilz, and R. Leberer, "A 77-GHz FM/CW radar front-end with a low-profile, low-loss printed antenna," *IEEE Trans. Microwave Theory Tech.*, vol. 47, pp. 2237–2241, 1999.

[7] W. Menzel, D. Pilz, and M. Al-Tikriti, "MM-wave folded reflector antennas with high gain, low loss, and low profile," *IEEE Antennas Propag. Mag.*, Jun. 2002.

[8] D. Pilz and W. Menzel, "Printed millimeter-wave reflectarrays," *Ann. Télécommun.*, vol. 56, no. 1-2, pp. 51–60, 2001.

[9] W. Menzel, M. Al-Trikriti, and R. Leberer, "A 76 GHz multibeam planar reflector antenna," in *Proc. Eur. Microwave Conf.*, vol. III, Milan, Italy, Sep. 2002, pp. 977–980.

[10] P. O. Savenko and V. J. Anokhin, "Synthesis of amplitude-phase distribution and shape of a planar antenna aperture for a given power pattern," *IEEE Trans. Antennas Propag.*, vol. 45, pp. 744–747, Apr. 1997.

[11] Y. Suzuki and T. Chiba, "An algorithm for pattern synthesis improvement," *IEEE Trans. Antennas Propag.*, vol. AP-34, pp. 825–829, Jun. 1986.

[12] T. Chiba, "On a pattern synthesis method for a linear array," *Proc. IEEE Int. Conv. Rec.*, no. 5, pp. 172–179, Mar. 1966.

[13] W. G. Jaeckle, "Antenna synthesis by weighted Fourier coefficients," *IEEE Trans. Antennas Propag.*, vol. AP-12, pp. 369–370, May 1964.

[14] P. M. Woodward, "A method for calculating the field over a plane aperture required to produce a given polar diagram," *Inst. Elec. Eng. J.*, vol. 93, no. IIIA, pp. 1554–1558, 1947.

[15] C. V. Baker, "A technique for the analytical synthesis of shaped beams for arrays," *IEEE Trans. Antennas Propag.*, vol. AP-17, pp. 803–805, Nov. 1969.

[16] W. L. Stutzman and E. L. Coffey, "Radiation pattern synthesis of planar antennas using the iterative sampling method," *IEEE Trans. Antennas Propag.*, vol. AP-23, pp. 764–769, Nov. 1975.

[17] R. Mittra and V. Galindo-Israel, "Some fundamental questions related to the problems of dual reflector synthesis," presented at the Proc. Nat. Radio Sci. Meeting, Boulder, CO, Jan. 1978.

Ralf Leberer received the Dipl.-Ing. and Dr.-Ing. degrees from the University of Ulm, Germany, in 1999 and 2005, respectively.

From 1999 to 2004, he was with the Department of Microwave Techniques, University of Ulm, as a Research Assistant. Since 2005, he has been with Microwave Factory/Research and Development, European Aeronautic Defence and Space (EADS) Company Deutschland GmbH, Ulm. His current areas of interest are quasi-planar reflectarrays, millimeter-wave sector and omnidirectional antennas, passive millimeter-wave components, and RF power amplifiers based on GaAs and GaN.

Wolfgang Menzel (M'89–SM'90–F'01) received the Dipl.-Ing. degree from the Technical University of Aachen, Germany, in 1974 and the Dr.-Ing. degree from the University of Duisburg, Germany, in 1977.

From 1979 to 1989, he was with the Millimeter-Wave Department, AEG (now Daimler-Chrysler Aerospace), Ulm, Germany. From 1980 to 1985, he was Head of the Laboratory for integrated millimeter-wave circuits. From 1985 to 1989, he was Head of the Millimeter-Wave Department. In that time, his areas of work included planar antennas, planar integrated circuits, and systems in the millimeter-wave frequency range. In 1989, he became a Professor at the University of Ulm. His current areas of interest are (multilayer) planar and waveguide circuits, antennas, millimeter-wave interconnects and packaging, and millimeter-wave system aspects.